HEFAT2007
5th International Conference on Heat Transfer, Fluid Mechanics and Thermodynamics
Sun City, South Africa
Paper number: MJ3

NUMERICAL SIMULATION OF FLUID FLOW, HEAT TRANSFER AND PRESSURE DROP IN THERMOPLATES

Mitrovic J.* and Maletic B.
*Author for correspondence
Department of Thermal Process Engineering and Plant Technology
University of Paderborn
33095 Paderborn
Germany
E-mail: mitrovic@tvt.upb.de

ABSTRACT

The objective of our investigations is to numerically investigate the optimal geometry of the thermoplate with respect to heat transfer of the inside fluid that passes through the channel as a single phase. In order to achieve this, the geometrical and process parameters such as the pattern of welding spots, the distance between the sheets, and the Reynolds number have been varied. For the simulation, the commercial software StarCD was used. The numerical experiments show that the heat transfer potential of the thermoplate having a staggered arrangement of welding spots is markedly higher than the one of a common flat channel, particularly at larger Reynolds numbers. The variations of the geometrical parameters indicate the welding spot pitch in a streamwise direction to be a pivotal quantity regarding the heat transfer optimisation.

INTRODUCTION

As heat transfer devices, thermoplates are encountered in several branches of engineering practice, e.g. as condensers or evaporators in thermal process technology and cooling techniques. In comparison to shell-and-tube heat exchanges, their installation is relatively simple, and the periphery is drastically reduced.

A thermoplate consists of two metallic sheets, which are spot-welded over the whole surface area according to an appropriate pattern, whereas the edges – except for connecting tubes – are continuously seam-welded. By applying a hydro-form technique, a channel that has a complex shape is established between the sheets, Figure 1. One fluid is conducted through this channel, the other one through the channel created by two neighbouring thermoplates that are assembled in parallel at certain spacing thus making a thermoplate heat exchanger.

One disadvantage of thermoplates lies in the fact that their thermo-fluid characteristic is scarcely explored, which prevents a reliable design of the corresponding heat exchangers.

We have not found relevant papers in the literature reporting on the experimental heat transfer and fluid flow characteristics of the interior, or the exterior fluid. The situation is much the same regarding the numerical experiments. An exception, to some extent, is a paper by Witry et al. [1], who numerically investigated the fluid flow and heat transfer in an automotive aluminium plate radiator provided with staggered, equidistantly arranged, dimples. On the contrary, there are numerous papers dealing with fluid flow and heat transfer in channels, or circular tubes, the walls of which were taken as sinusoidally shaped, see e. g. [2-11], to name only a few.

NOMENCLATURE

d	[m]	Equivalent plate distance
d_h	[m]	Hydraulic diameter
h_m	[W/m^{2}K]	Average heat transfer coefficient
k	[W/mK]	Thermal conductivity
$\mathbf{n}$	[-]	Normal unit vector
Nu_m	[-]	Average Nusselt number
P	[W]	Pumping power
p_{IN}	[bar]	Inlet pressure
p_m	[bar]	Average pressure
p_{OUT}	[bar]	Outlet pressure
$\dot{q}_m$	[W/m^2]	Average heat flux
s_L	[m]	Streamwise welding spot pitch
s_T	[m]	Spanwise welding spot pitch
T_b	[K, °C]	Fluid bulk temperature
T_{IN}	[K, °C]	Fluid inlet temperature
T_W	[K, °C]	Wall temperature
$\mathbf{w}$	[m/s]	Velocity vector
U	[m]	Circumference of channel cross-section
$(\dot{Q}/P)_{TP}$	[-]	Thermo-hydraulic characteristic of thermoplate
$(\dot{Q}/P)_{FC}$	[-]	Thermo-hydraulic characteristic of flat channel
x_0, z_0	[m]	Coordinates of welding spot centres

Special characters

δ	[m]	Maximal plate distance
ε	[m]	Size of numerical cell

Motivation for these studies was mainly rooted in the desire to quantify the transport mechanisms in fluid flowing past wavy walls in comparison to conduits having even walls. Different fluid flow models and numerical techniques as well were employed and several details on the flow field were reported. Commonly, complex velocity fields with flow separations and reattachments with recirculation zones were observed. Cherukat et al. [3], applying the direct numerical simulation with fully developed turbulent flow along a two-dimensional wavy wall, were able to identify several modes of the wall-fluid interactions which allow deeper insights into the flow structure and heat transfer mechanisms. Although the works mentioned above are performed with two-dimensional flows on a macroscopic scale, they provide fundamental background information that is basically also valid for our numerical experiments performed for channels with a pronounced three-dimensional flow.

SCOPE OF THE PAPER

The present paper is based on a conference contribution [12]. Its objective is to numerically obtain the sets of the geometrical parameters that, in interaction with process parameters, should pave the way for optimal heat transfer of the inside fluid which is assumed to pass the thermoplate as a single phase (coolant in Figure 1). The geometry of the simulated three-dimensional domain is shown in Figure 2. It consists of a strip of a thermoplate channel, the latter being unbounded in spanwise (z) direction. The semi-circles represent the welding spots, which are arranged in a staggered manner. The strip is confined in a spanwise direction by the planes $z = 0$ and $z = s_T$, and in a streamwise (x) direction by $x = 0$ and $x = L$.

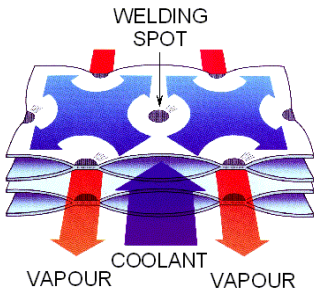

Figure 1 Fluid flow arrangement in thermoplates (DEG-Engineering).

The heat transfer surface area is considered to be a three-dimensional mathematical surface represented by

$$y = \frac{\delta}{4}\left(1+\cos\left(\frac{z}{s_T}\pi\right)\cos\left(2\frac{x}{s_L}\pi\right)\right), \qquad (1)$$

where the geometrical parameters can be taken from Figure 2. The computational domain is determined by the surface $y = f(x,z)$ according to the equation (1), the planes $x = 0$ and $x = L$, the symmetry planes $z = 0$, $z = s_T$, $y = 0$, and the cylindrical surface,

$$(x - x_0)^2 + (z - z_0)^2 = R^2, \qquad (2)$$

where x_0 and z_0 are the centres of the welding spots obtained as the roots of the equation $y = f(x,z) = 0$. In this context, it should be noted that the mathematical contour of the thermoplate according to the equation (1) does not ideally represent the reality, but the discrepancy as regards the thermo-hydraulic behaviour of the system is expected to be of marginal importance. Moreover, in reality, the welding spots act thermally as circular fins with a minimal drawing temperature difference in their centres.

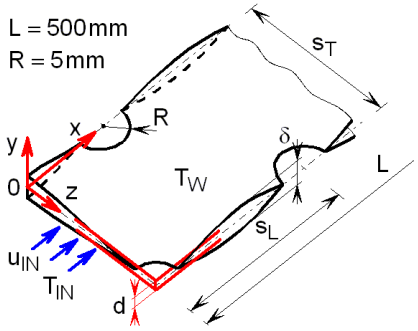

Figure 2 Geometry and dimensions of the three-dimensional simulated domain

In the simulations, the geometrical parameters, such as the streamwise and the transversal welding spots pitch, s_L and s_T, and the maximal distance between the metallic sheets, δ, have been varied, whereas the radius, R, of the welding spots was kept constant. To obtain some insights into the flow and temperature fields in the developing region, a relatively short length, L, of the strip was first chosen. This length was then gradually increased up to $L = 500\ mm$, and, at a low fluid velocity, the fully developed region was included into the simulation domain. The distance, δ, and the Reynolds number, Re, that is formed with the fluid inlet velocity, u_{IN}, have also been varied. The fluid inlet temperature, T_{IN}, and the wall temperature, T_W, were taken to be constant.

GOVERNING EQUATIONS AND BOUNDARY CONDITIONS

The fluid flow was considered to be laminar, incompressible, stationary and three-dimensional. Water of constant physical properties is adopted for the numerical experiments. The velocity and the temperature fields are governed by the equations of continuity, momentum and energy:

$$\nabla \cdot \mathbf{w} = 0, \qquad (3)$$

$$\nabla \cdot \rho \mathbf{ww} = -\nabla p + \mu \nabla^2 \mathbf{w}, \qquad (4)$$

$$\rho c_p \mathbf{w} \nabla T = k \nabla^2 T + \mu \Phi, \qquad (5)$$

where ρ denotes the fluid density, μ the dynamic viscosity, c_p

the specific heat capacity, k the thermal conductivity, $\mathbf{w}$ the velocity vector, T the temperature, p the pressure, and Φ the dissipation function.

The model equations (3-5) were treated numerically subject to the boundary conditions:

$$y = f(x,z): \mathbf{w} = 0,\ T = T_{\mathrm{W}};\quad y = 0: \frac{\partial \mathbf{w}}{\partial y} = 0,\ \frac{\partial T}{\partial y} = 0, \tag{6}$$

$$z = 0: \frac{\partial \mathbf{w}}{\partial z} = 0,\ \frac{\partial T}{\partial z} = 0;\qquad z = s_T: \frac{\partial \mathbf{w}}{\partial z} = 0, \frac{\partial T}{\partial z} = 0, \tag{7}$$

$$x = 0: \mathbf{w} = \{u_{\mathrm{IN}}, 0, 0\}, T = T_{\mathrm{IN}};\quad x = L: \frac{\partial \mathbf{w}}{\partial x} = 0, \frac{\partial T}{\partial x} = 0. \tag{8}$$

The momentum and heat transfer in the streamwise direction at $x = L$ are neglected in the boundaryconditions (8). Clearly, this simplification is not strictly fulfilled in reality, but the errors thus introduced affect the corresponding fields only in the immediate vicinity of the channel outlet.

In the numerical simulations, the commercial software *StarCD* was utilised [13].

PROCESS QUANTITIES

Once the governing equations are solved and the flow and temperature fields are obtained, the fluid bulk temperature (the mixing cup temperature), $T_{\mathrm{b}}(x)$, and the local wall heat flux, $\dot{q}(x)$, averaged in a spanwise (z) direction, can be calculated by

$$T_{\mathrm{b}}(x) = \int_S uT dS \Big/ \int_S u dS, \tag{9}$$

$$\dot{q}(x) = \frac{1}{A_{\mathrm{S}}} \int_{A_{\mathrm{S}}} (\dot{\mathbf{q}} \cdot \mathbf{n}) dA_{\mathrm{S}}, \tag{10}$$

where $S = S(x)$ represents the cross-sectional flow area of the channel, A_{S} a narrow strip of the surface $y = f(x,z)$ bounded by the planes $x - (\varepsilon/2)$ and $x + (\varepsilon/2)$, ε being the width of the numerical cell in the x-direction.

The average wall heat flux, $\dot{q}_{\mathrm{m}}(x)$, and the heat flow rate, $\dot{Q}(x)$, are obtained in a similar way:

$$\dot{q}_{\mathrm{m}}(x) = \frac{1}{A} \int_A (\dot{\mathbf{q}} \cdot \mathbf{n}) dA;\ \dot{Q}(x) = \int_A (\dot{\mathbf{q}} \cdot \mathbf{n}) dA, \tag{11}$$

where A denotes the surface area extending the distance x in the streamwise direction from the inlet.

The local heat transfer coefficient, $h(x)$, is defined by

$$h(x) = \frac{\dot{q}(x)}{T_{\mathrm{W}} - T_{\mathrm{b}}(x)}, \tag{12}$$

with $T_{\mathrm{b}}(x)$ and $\dot{q}(x)$ according to equations (9) and (10); T_{W} represents the wall temperature.

The average heat transfer coefficient, $h_{\mathrm{m}}(x)$, and the average Nusselt number, Nu_{m}, are obtained from

$$h_{\mathrm{m}}(x) = \frac{1}{x} \int_0^x h(x) dx;\ \mathrm{Nu}_{\mathrm{m}} = \frac{h_{\mathrm{m}} d_{\mathrm{h}}}{k}, \tag{13}$$

with d_{h} as the hydraulic diameter,

$$d_{\mathrm{h}} = \frac{4S}{U} = 2d;\ d = \frac{V}{s_{\mathrm{T}} L}, \tag{14}$$

S being the cross-sectional flow area, U its circumference, and d the distance between the parallel plates of a channel having the same volume V as the actual thermoplate, Figure 2. Note that the hydraulic diameter d_{h} defined in this way does not change along the channel length.

A further quantity involved in the presentation of the results is the Reynolds number,

$$\mathrm{Re} = \frac{u d_{\mathrm{h}}}{\nu}, \tag{15}$$

where u is the average axial velocity component, and ν the kinematic viscosity.

In order to obtain a thermo-fluid characteristic of the thermoplate, the local pressure, $p_{\mathrm{m}}(x)$, averaged along the coordinates y and z, and the pumping power, P, are calculated as follows

$$p_{\mathrm{m}}(x) = \frac{1}{S} \int_S p dS, \tag{16}$$

$$P = (p_{\mathrm{IN}} - p_{\mathrm{OUT}}) \dot{V}, \tag{17}$$

where $p_{\mathrm{IN}} = p_{\mathrm{m}}(0)$ and $p_{\mathrm{OUT}} = p_{\mathrm{m}}(L)$ are the averaged inlet and outlet pressure, respectively, and $\dot{V}$ denotes the volume flow rate.

RESULTS

Because of the complex geometry of the computational domain, all the non-scalar quantities obtained from the governing equations are three-dimensional. This poses some difficulties on the presentation of the results. For this reason, the interesting quantities will be visualised in the following sections as general images and quantitatively illustrated in characteristic planes, or on surfaces.

The velocity field

Figure 3 shows the development of the velocity field in the symmetry plane $y = 0$ for a larger Reynolds number $\mathrm{Re} = 3800$ adopted in the numerical experiments. At this Reynolds number, fluid separation establishes between the welding spots with reattachments at the contour of the neighbouring, downstream spots, and a comparatively large portion of the channel is occupied by recirculation zones. These zones are responsible for local fluid acceleration. In the middle of the channel, there is a meandering fluid core that only touches the welding spots since it is bounded by the recirculation zones. Similar flow structures have been reported in [11], on the basis

of the numerical experiments, and in [14, 15] in laboratory experiments, using two-dimensional channels in all cases.

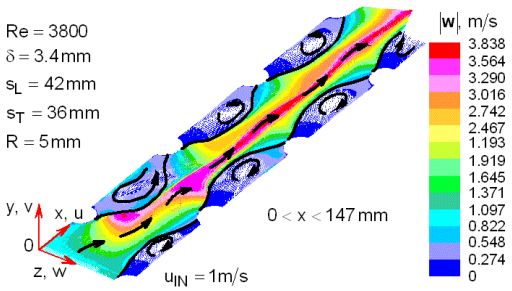

Figure 3 Velocity field in the plane $y = 0$ at $\mathrm{Re} = 3800$; for geometry see Figure 2.

From Figure 3 one might infer that in the same cross-section turbulent flow may coexist with the laminar flow. The extension of one flow mode occurs at the expenses of the other one, and turbulence will occupy the larger portion of the channel cross-section, the larger being the Reynolds number. The curvature of the boundary is expected to support the generation of Görtler's vortices and hairpin vortex structures, see e.g. [5]. In this context it is to be noted that possible laminar-turbulent flow transitions are disregarded in our simulations.

The temperature field and heat transfer

Figure 4 gives some insights into the development of the temperature field in the *x*0*z* symmetry plane of the channel. The fluid is heated by the plates, which are kept isothermal at $T_W = 333\,K$. At $\mathrm{Re} = 3800$ the fluid in the central portion of the strip remains thermally unaffected by the heating plates, and the thermally developing region occupies a channel length of about $3 \cdot s_L$. In the recirculation zones (Figure 3), the fluid approaches the temperature of the wall much faster.

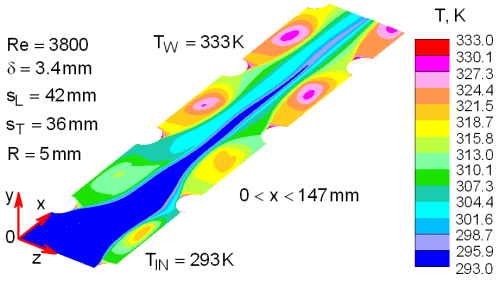

Figure 4 Temperature field in the plane $y = 0$ at $\mathrm{Re} = 3800$; for geometry see Figure 2.

The distribution of the heat flux as a vector intensity $|\dot{\mathbf{q}}|$ is illustrated in Figure 5. The heat flux is seen to decrease in a streamwise (*x*) direction, becoming smaller in the recirculation zones than in the central part of the strip. The heat flux fluctuates significantly not only spanwise, but also in a streamwise direction. The positions of the maxima nearly coincide with the axial positions of the welding spots.

The distributions of the heat transfer coefficients, $h(x)$ and $h_m(x)$, according to equations (12) and (13), are demonstrated in Figure 6. The quantity $h(x)$ behaves oscillatory damped along the channel, decaying at the same time both in amplitude and magnitude.

This behaviour of the heat transfer coefficient, $h(x)$, is qualitatively comparable with the corresponding ones reported in [5, 8, 9, 10] for two-dimensional channels.

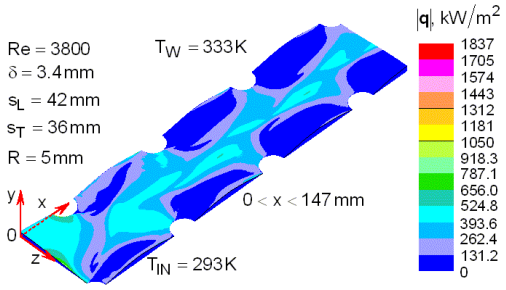

Figure 5 Wall heat flux field at $\mathrm{Re} = 3800$

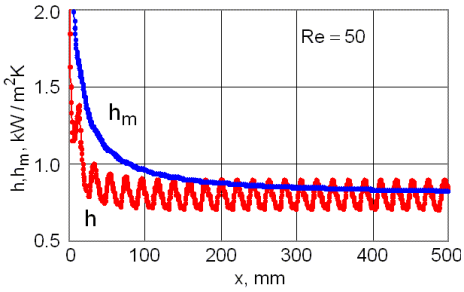

Figure 6 Wall heat flux field at $\mathrm{Re} = 3800$

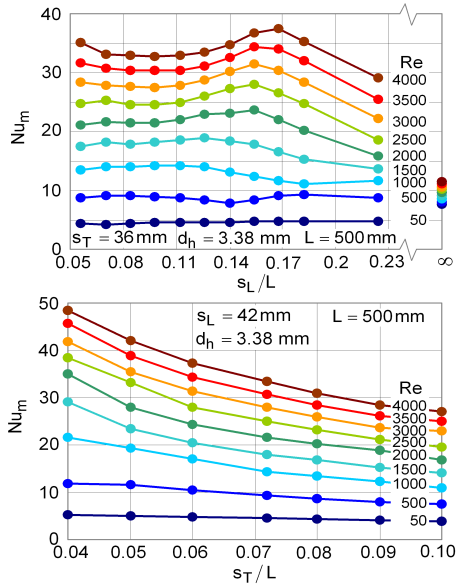

Figure 7 Average Nusselt number of a 500 *mm* long channel at different Re as function of s_L/L and s_T/L ($s_L/L \to \infty$: parallel plates), and d_h/L

If the longitudinal and the transversal pitch of the welding spots, s_L and s_T, are varied, the distribution of the Nusselt number and of the corresponding heat transfer coefficient, equation (13), are very similar. Therefore only the quantity Nu_m is displayed in Figure 7.

As may be taken from the diagram, a larger Reynolds number corresponds to a larger Nusselt number, i.e. heat transfer coefficient. At the smallest Reynolds number, the heat transfer is largely independent of s_L and s_T, whereas at other values of Re, certain dependency of Nu_m on s_L and s_T is observed. At $s_L \to \infty$, Nu_m tends towards the values for the channel formed by plane parallel plates. These values are higher than the ones for the thermoplate at smaller Re. The situation reverses at larger Re, where the heat transfer of the themoplate becomes better. Whereas the quantity Nu_m is steadily decreasing with increasing s_T, certain maxima of Nu_m are observed at $s_L \approx 80\,mm$ at larger Reynolds numbers. This conclusion is valid only for the parameters noted in the diagrams.

The heat transfer coefficient h_m and the Nusselt number Nu_m as functions of the hydraulic diameter d_h and d_h/L, respectively are displayed in Figure 8. The decrease of the heat transfer coefficient h_m with increasing d_h is rooted in a corresponding reduction of the fluid velocity at the given Reynolds number. The increase of Nu_m with increasing d_h/L is associated with the increase of d_h.

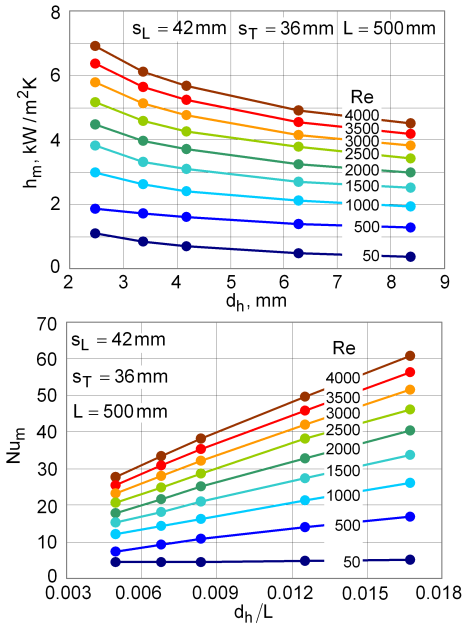

Figure 8 Average heat transfer coefficient and Nusselt number of a 500 *mm* long channel at different Re as function of of hydraulic diameter d_h and the ratio d_h/L, respectively

In summary, the parameter variations clearly show the Nusselt number to depend on the geometrical quantities of the thermoplate and the fluid velocity. The results obtained from the present state of our numerical experiments do, however, not suffice to recommend a more comprehensive correlation for the heat transfer. This requires variation of other important parameters, such as the radius and shape of the welding spots, the length of the plate and the Prandtl number.

The thermo-fluid characteristic

The complex geometry of the thermoplate channel results in a larger heat transfer coefficient in comparison to the channel with plane walls. This heat transfer improvement is to be paid by a larger pressure drop, that is to say, by a larger pumping power at given volume flow rate. To illustrate this interplay, one usually combines the heat flow rate, $\dot{Q}$, and the pumping power, P, to a thermo-fluid characteristic of the heat transfer device, see e.g. Stephan and Mitrovic [17], and Webb [18]. For instance, the ratio $\dot{Q}/P$ specifies the running costs of the heat transfer.

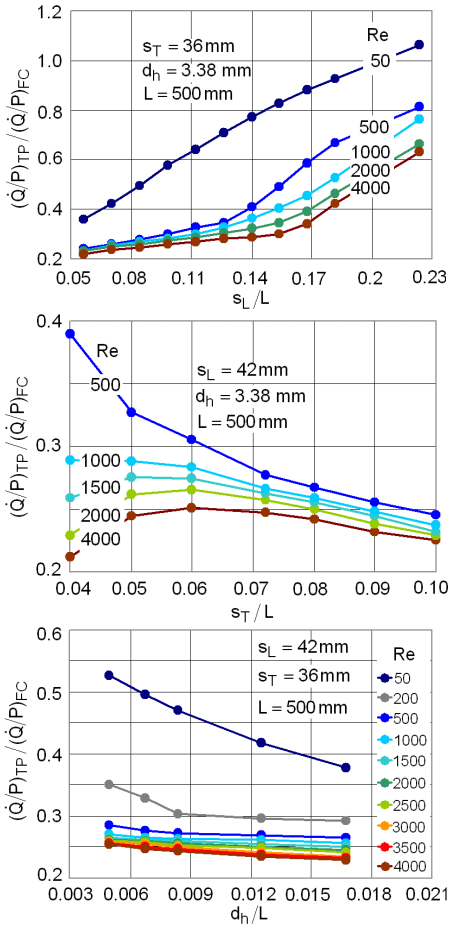

Figure 9 Thermo-fluid characteristic of the thermoplate compared with the characteristic of the flat channel at selected Reynolds numbers

Figure 9 shows the ratio of the thermo-fluid characteristics $(\dot{Q}/P)_{TP}$ and $(\dot{Q}/P)_{FC}$ of the thermoplate and of the flat

channel with plane walls as function of the geometrical parameters for selected Reynolds numbers, Re. The ratio is seen to increase with increasing s_L/L, but it still remains smaller than unity, the curve for $\mathrm{Re} = 50$ at larger s_L/L being an exception.

In general, at a larger Reynolds number the thermoplate is more effective than at smaller ones. Furthermore, the ratio $(\dot{Q}/P)_\mathrm{TP}/(\dot{Q}/P)_\mathrm{FC}$ is smaller at smaller s_L/L and larger d_h/L. Its dependency on s_T/L is more complicated because of the maxima at larger Reynolds numbers.

Summarizing the results on thermo-fluid characteristic, we may conclude that the flat channel formed by plane walls shows a better heat transfer characteristic, expressed in terms of pumping power, than the corresponding thermoplate. However, a fabrication of such a channel without welding spots seems scarcely possible in sizes required in common practice and, from this point of view, the parallel plate channel serves merely as a model for comparison purposes.

CONCLUSION

Thermoplates are efficient heat transfer devices, which are used in several branches of engineering practice. The complex geometry of the inside channel of such a plate results in a flow field with a pronounced three-dimensional character. Our comprehensive, and at present, not finished investigations aim at obtaining a better understanding of the inside fluid flow and heat transfer, in order to develop a more powerful relationship for heat transfer, including also the pressure drop, which could serve as indicators when trying to optimise the channel geometry with respect to the thermo-fluid characteristic of the thermoplate.

Despite the fact that not all of the parameters have been varied in the range required for the practical purposes, the results obtained are conclusive regarding the heat transfer potential of the thermoplate in comparison to a flat channel with plane walls. Depending on the geometrical and process parameters, the heat transfer improvement in the thermoplate ranges almost up to the factor of 4. However, this improvement has to be paid by an increased pressure drop resulting in a larger pumping power at the same fluid flow rate. Moreover, the computer simulations have revealed that the recirculation zones, establishing behind the welding spots, sensitively affect the heat transfer and pressure drop in a manner which worsens the thermo-fluid characteristic of the thermoplate. Further numerical simulations should also provide the information on the arrangement and shape of the welding spots and pave the way in how to shape the thermoplate and to optimise its heat transfer characteristic.

REFERENCES

[1] Witry A., Al-Hajeri M.H., and Bondok A.A., Thermal performance of automotive aluminium plate radiator, *Applied Thermal Engineering*, Vol. 25, 2005, pp. 1207-1218

[2] Burns J.C., and Parkes T., Peristaltic motion, *Journal of Fluid Mechanics*, Vol. 29, 1967, pp.731-743

[3] Cherukat P., Na Y., Hanratty T.J., and Mclaughlin Y.B., Direct numerical simulation of a fully developed turbulent flow over a wavy wall, *Theoretical and Computational Fluid Dynamics*, Vol 11, 1998, pp. 109-134

[4] Dellil A.Z., Azzi A., and Jubran, B.A., Turbulent flow and convective heat transfer in a wavy wall channel, *Heat and Mass Transfer*, Vol 40, 2004, pp. 793-799.

[5] Garg V.K., and Maji P.K., Laminar flow and heat transfer in a periodically converging-diverging channel, *International Journal of Numerical Methods in Fluids*, Vol. 8, 1988, pp. 579-597

[6] Hossain M.Z., and Islam A.K.M.S., Fully developed flow structures and heat transfer in sine-shaped wavy channels, *International Communications in Heat and Mass Transfer*, Vol. 31, 2004, pp. 887-896

[7] Mahmud S., Islam A.K.M.S., and Feroz C.M., Flow and heat transfer characteristic inside a wavy tube, *Heat and Mass Transfer*, Vol. 39, 2003, pp. 387-393

[8] Russ G., and Beer H., Heat transfer and flow field in a pipe with sinusoidal wavy surface – I. Numerical investigation, II. Experimental investigation, *International Journal of Heat and Mass Transfer*, Vol. 40, 1997, pp.1061-1081

[9] Saniei N., and Dini, S., Heat transfer characteristics in wavy-walled channel, *ASME Journal of Heat Transfer*, Vol. 115, 1993, pp. 788-792

[10] Wang C.C., and Chen C.K., Forced convection in a wavy-wall channel, *International Journal of Heat and Mass Transfer*, Vol. 45, 2002, pp. 2587-2595

[11] Wang G., and Vanka S.P., Convective heat transfer in periodic wavy passages, *International Journal of Heat and Mass Transfer*, Vol. 38, 1995, pp. 3219-3230

[12] Mitrovic J., and Maletic B., Numerical simulation of fluid flow and heat transfer in thermoplates, *Proceedomgs pf the 13th International Heat Transfer Conference*, Sydney, Australia, Paper HEX-10, August 2006

[13] CD adapco Group. 2004. Methodology StarCD version 3.24

[14] Nishimura T., Murakami S., Arakawa S., and Kawamura Y., Flow observation and mass transfer in sinusoidal wavy-walled channel at moderate Reynolds numbers for steady flow, *International Journal of Heat and Mass Transfer*, Vol. 33, 1990, pp. 835-845

[15] Rush T.A., Newell T.A., and Jacobi, A.M., An experimental study of fluid flow and heat transfer in sinusoidal wavy passages, *International Journal of Heat and Mass Transfer*, Vol. 42, 1999, pp. 1541-1553

[16] Grass A.J., Stewart R.J., and Mansour-Tehrani M., Vortical structures and coherent motion in turbulent flow over smooth and rough boundaries, *Philosophical Transactions of the Royal Society of London, Series A*, Vol. 336, 1991, pp 35-65

[17] Stephan K., and Mitrovic J., Measures for Enhancement of Heat Transfer, in German, *Chemie-Ingenieur-Technik*, Vol. 56, 1984, pp. 427-431

[18] Webb R.L., Principles of enhanced heat transfer, New York, Wiley, 1994.